Research Square

Preprints are preliminary reports that have not undergone peer review.
They should not be considered conclusive, used to inform clinical practice,
or referenced by the media as validated information.

Tracking excited state decay mechanisms of pyrimidine nucleosides in real time

Giulio Cerullo (giulio.cerullo@polimi.it)
Politecnico di Milano https://orcid.org/0000-0002-9534-2702
Rocio Borrego-Varillas
Politecnico di Milano https://orcid.org/0000-0002-4499-0558
Artur Nenov
Università degli Studi di Bologna
Piotr Kabacinski
Politecnico di Milano https://orcid.org/0000-0003-4591-5100
Irene Conti
Università degli Studi di Bologna
Lucia Ganzer
Politecnico di Milano
Aurelio Oriana
Politecnico di Milano
Ines Delfino
Università della Tuscia
Oliver Weingart
Heinrich Heine Universität Düsseldorf
Cristian Manzoni
Politecnico di Milano
Ivan Rivalta
Università degli Studi di Bologna
Marco Garavelli
Università di Bologna

Article

Keywords: Photostability, Electronic Energy Dissipation, Transient Absorption Spectroscopy, Quantum Dynamics Simulations, Lesion-inducing Coordinates

Posted Date: November 18th, 2020

DOI: https://doi.org/10.21203/rs.3.rs-97259/v1

License: This work is licensed under a Creative Commons Attribution 4.0 International License.
Read Full License

Version of Record: A version of this preprint was published at Nature Communications on December 14th, 2021. See the published version at https://doi.org/10.1038/s41467-021-27535-7.

Abstract

DNA owes its remarkable photostability to the ability of its building blocks – the nucleosides – to efficiently dissipate the excess electronic energy acquired upon photoexcitation with ultraviolet light. The exact mechanism occurring on a sub-picosecond time scale has been a matter of intense debate. Here we combine sub-30-fs transient absorption spectroscopy with broad spectral coverage and state-of-the-art quantum dynamics simulations to resolve the early steps of the deactivation mechanisms of uridine (Urd) and 5-methyluridine (5mUrd) in aqueous solution. For both nucleosides we track the wave packet motion from the Franck-Condon region to the conical intersection (CI) with to the ground state and observe a direct spectral signature of an excited-state vibrational mode leading to the CI. We find that 5mUrd exhibits an order of magnitude longer excited state lifetime with respect to Urd and assign it to the larger inertia of the methyl group involved in the ring puckering mode leading to the CI. We argue that this longer lifetime enables the activation of potentially lesion-inducing coordinates such as ring opening, elucidating the origin of the susceptibility of thymine-containing DNA strands to photodamage.

Introduction

Ultraviolet (UV) radiation can induce significant photodamage to biomolecules. This is particularly true for nucleotides, the building blocks of DNA, which display strong absorption bands in the UV. Due to the high energy of the UV photons, the excess electronic energy acquired by the molecule could initiate a chain of photochemical reactions ultimately altering the structure of the base sequence[1–4]. In particular, pyrimidine dimerization leads to covalent linkage of two adjacent thymine (also known as 5-methyluracil) bases, forming the cyclobutane pyrimidine dimer, which is believed to trigger carcinogenesis[5–10]. However, remarkably, in most cases photoexcitations in DNA do not trigger reactions, because electronic energy undergoes efficient non-radiative dissipation on ultrafast timescales ranging from sub-picosecond [11–16] in isolated nucleotides to few hundreds of picoseconds in base pairs, single strands and double stranded DNA, resulting in effective photoprotection mechanisms[17–20].

Although multiple scenarios have been proposed[17,19], it is now generally accepted that conical intersections (CIs) play a crucial role in the deactivation pathways of nucleotides[21] and are responsible for the ultrafast internal conversion (IC) to the ground state. However, no consensus has been reached yet on the decay mechanisms. In particular, in pyrimidines, the time scale of IC and the involvement of intermediate dark states are still disputed. Experimental transient absorption (TA), photo-electron spectroscopy and fluorescence up-conversion measurements on pyrimidines and their nucleosides in aqueous solution agree on the early fate of the initially excited (ππ*) singlet state, that decays with one or two sub-picosecond components[12,14,22–29] and a further component of several picoseconds[12–14,22–27,30–33]. The sub-picosecond decay has been assigned to direct IC to the ground state and/or to a dark (nπ*) singlet excited state, whereas the long component has been attributed to various mechanisms including ground state vibrational cooling, intersystem crossing (ISC) to triplet states, IC of dark states to the ground state or population trapping in the ππ* state. A review of the different hypotheses and

experimental time constants is provided in Supplementary Note 1. Thus, key questions regarding the assignment of the experimental decay times, the involvement of dark states, and the molecular processes responsible for the higher reactivity of thymine, remain open.

Experimental and theoretical bottlenecks have so far hindered unambiguous definition of the molecular mechanisms underlying pyrimidine excited state deactivation. From an experimental point of view, the lack of temporal resolution and the limited spectral coverage of the probe pulses have prevented an accurate tracking of dynamics taking place on the sub-100-fs timescale. From a theoretical point of view, simulations of excited states dynamics have been mostly carried out in semi-classical fashion, sacrificing accuracy either by neglecting the environmental effects (i.e. assuming vacuum environment) or by adopting quantum-mechanical (QM) treatments of the electronic structures, with limited description of electronic correlations.

Here we perform TA spectroscopy in the pyrimidine nucleosides uridine (Urd) and 5-methyluridine (5mUrd) in aqueous solution with ~30-fs temporal resolution, which exceeds by almost one order of magnitude that of previous studies, and full coverage of the 1.9-4.2 eV probe spectral range. Combining the experimental results with simulations based on mixed quantum-classical dynamics within a hybrid quantum mechanics/molecular mechanics (QM/MM) framework explicitly including environmental effects and electronic correlation, we are able to unambiguously assign the observed spectral signals and the corresponding time constants to the specific pathways responsible for the decay.

Our results show that, in both Urd and 5mUrd, IC through ring puckering is the main decay mechanism to the ground state, but 5mUrd takes an order of magnitude longer (»1 ps versus »100 fs) to reach the crossing region. Based on our model, we explain the longer lifetime of 5mUrd with the larger inertia of the group involved in the ring puckering (methyl in 5mUrd with respect to hydrogen in Urd), rather than with a difference in the potential energy surface (PES) of the photoactive (ππ*) state. We find experimental and theoretical evidence for the partial population of the dark nπ* state in Urd, whereas we do not find any evidence for its involvement in 5mUrd. Our model shows that, as a consequence of the longer lifetime of the bright ππ* state, 5mUrd explores other deactivation routes (C_4=O_8 out-of-plane bending and N_1-C_2 ring-opening), thus accounting for the enhanced lesion susceptibility of thymine-containing polynucleotides.

Results And Discussion

Transient absorption spectra of pyrimidines

Figure 1d shows TA spectra of Urd in phosphate buffer solution, recorded with sub-30-fs temporal resolution[34,35] following photoexcitation at 4.5 eV. At early times we observe an intense stimulated emission (SE) band in the UV, covering the 3.00-4.00 eV spectral range, as well as a photoinduced absorption (PA) feature below 2.4 eV (PA_1). An additional PA band can be observed at early times at 3.10 eV for orthogonal pump and probe polarizations (Supplementary Fig. S33), which is covered by the SE for

parallel polarizations (Fig. 1c). Both the SE and PA_1 bands decay very quickly and completely vanish after ~200 fs, giving rise to another PA band (PA_2) at longer times covering the entire near-UV spectral window (3.10-4.25 eV). By fitting the SE dynamics with a bi-exponential function (with a long component fixed as offset in order to describe dynamics at times beyond our temporal window) we obtain a fast decay time of ~80 fs, whereas this constant increases to ~125 fs for PA_1 (see Supplementary Fig. 41).

The TA maps of 5mUrd, shown in Fig. 2, are qualitatively similar to those of Urd. At early times, we observe a SE signal in the UV region, confined in the 3.35-4.00 eV window, as well as a PA band extending below 2.4 eV (PA_1) and a second one above 4 eV (PA_2). As in Urd, an additional PA band is observed at 3.10 eV for crossed pump and probe polarizations (Supplementary Fig. S35). The key difference with respect to Urd is in the spectral dynamics of these features. The SE exhibits a clear red-shift during the first 200 fs accompanied by a significant broadening (see TA spectra in Supplementary Fig. S29). At 3.60 eV the SE band is characterized by a bi-exponential decay with a fast ~70 fs component and a slower tail featuring a 770 fs time constant. At 2 eV PA_1 is characterized by comparable decay times of 135 fs and 1.16 ps (see Supplementary Fig. S41). On the other hand, the PA_2 band exhibits a delayed build-up in the first 100 fs which correlates to the dynamics of the SE. This rise is due to the red-shift of the SE band that uncovers the underlying PA. Subsequently, it decays on a few ps time scale accompanied by a blue-shift.

Uridine decays ballistically to the ground state through a ring puckering channel

To interpret the observed ultrafast relaxation dynamics, we compare them to virtual TA spectroscopy maps computed from first principles. We use a mixed quantum-classical dynamics approach in a QM/MM framework, that couples a multireference dynamically correlated description (CASPT2) of the pyrimidine nucleobase with an explicit classical atomistic model (AMBER force field) of the environment (sugar substituents and solvent). Further details are provided in Supplementary Note 2.

Figure 1c reports the computed TA spectra of Urd, which are in striking agreement with experiment with the exception of a systematic blue shift by »300 meV (also observed for 5mUrd). We assign the SE and PA_1 signals at early times to the ππ* state. Simulations with cross-polarized pump and probe pulses (Supplementary Fig. S33), as well as “PA only” spectra (Supplementary Fig. S36) reveal an additional PA band at early times around 3.40 eV, in agreement with the experiment. PA_2 is clearly identified as PA from the hot ground state. By fitting the population dynamics of the ππ* state (Fig. 1b) with a mono-exponential function, we obtain a lifetime of 120 fs which compares well to the lifetime obtained by fitting both the experimental (125 fs) and the modelled (110 fs) spectral dynamics of the PA_1 band at ~2 eV.

Through static computations within the hybrid QM(CASPT2)/MM(AMBER) framework we recently identified two deactivation channels from the lowest bright ππ* state to the ground state in pyrimidine nucleosides, involving ring-puckering with H_9 out-of-plane bending and N_1-C_2 bond breaking[36]. Both deactivation pathways are associated with CIs reached over small barriers (0.1-0.2 eV), making them potentially responsible for the ballistic ~100 fs decay observed experimentally. Our mixed quantum-

classical dynamics simulations enable us to identify ring puckering as the largely dominant excited state deactivation mechanism in Urd with excitation at 4.5 eV (Supplementary Note 3.6.1).

The origin of the fast and slow sub-picosecond components in the spectra of 5-methyluridine: relaxation from the Franck-Condon region and internal conversion to the ground state

The observed analogy in the overall appearance of the ultrafast TA spectra of Urd and 5mUrd is understood by the rather similar electronic structure of both nucleobases. This is also confirmed by the simulations of 5mUrd, which reproduce all relevant features (Fig. 2c) within the margin of error. The simulations recover the red-shift of the SE during the first 300 fs, which is accompanied by the rise of PA_2 above 4.00 eV (above 3.70 eV in the experimental spectrum in Fig 2C). “PA only” spectra assign this signal to the tail of an intense PA band of the ππ* state (Supplementary Fig. S37), revealed only upon red-shift of the overlapping SE signal. With time, the PA of the ππ* state is progressively overlaid by the PA of the hot ground state which becomes the dominant feature only after about 700-800 fs, thus rationalizing the apparent long lifetime of the PA_2 band in comparison to the remaining fingerprint bands of the ππ* state. Two additional PA bands characterize the ππ* state at early times, PA_1 below 2.10 eV, clearly visible in the simulated spectrum, and another one peaking at 3.30 eV, whose tail at 3 eV is faintly visible in the spectrum during the first 100 fs and is clearly resolved in cross-polarized spectra (Supplementary Fig. S35). Upon red-shift the SE overlaps with both PA bands, leading to the ultrafast disappearance of the band at 3.30 eV and to pronounced intensity fluctuations in PA_1, which nevertheless survives until the end of the simulation time window.

The non-adiabatic dynamics underlying the simulated spectra reveals a surprising picture. The lowest ππ* state of 5mUrd is found to decay on a time scale of several hundred fs (a mono-exponential fit of the population dynamics in Fig. 2b reveals a lifetime of 750 fs), which is almost one order of magnitude longer than Urd. Moreover, only one hopping event is encountered during the first 200 fs. Thus, it is not the fast component observed in the TA spectra (Fig. 2c) that is to be associated with the decay to the ground state, but rather the slower component. In the light of our analysis, the ultrafast ~100 fs component obtained by fitting the dynamics of the SE and PA_1 does not arise from ultrafast depopulation of the ππ* state, but rather from: i) the spectral red-shift due to wave packet departure from the Franck-Condon (FC) region; ii) the spectral diffusion associated with the extremely flat excited state PES; iii) destructive overlap between the SE and PA bands.

Internal conversion mechanism of 5-methyluridine: towards a comprehension of its higher reactivity

After 1 ps about 20% of the trajectories in 5mUrd are found to still roam in the excited state PES. As for Urd, ring-puckering is found to be the dominant deactivation pathway, channelling about 90% of the decaying population; however, this time the puckering mode involves the methyl group (Supplementary Note 3.6.2). Accordingly, the difference in excited state lifetimes between Urd and 5mUrd is attributed to the larger inertia of the methyl group. A few trajectories are found to explore O_8-out-of-plane bending during deactivation and a single trajectory undergoes N_1-C_2 bond breaking, thus confirming the feasibility

of the ring-opening route (Supplementary Note 3.6.2). The longer excited state lifespan of 5mUrd facilitates the activation of diverse conformational degrees of freedom, which renders it potentially more prone to photodamage. In this regard, it is well known that thymine is responsible for the formation of cyclobutane pyrimidine dimers and 6-4 photoproducts[8]. The higher reactivity of 5mUrd is thus consistent with our finding that the nucleoside does not decay to the ground state in a ballistic fashion, but rather is allowed to explore various deactivation routes thanks to the longer lifetime.

Involvement of the np* state in the deactivation of uridine and 5-methyluridine

Could an ultrafast non-adiabatic transfer to a non-emitting excited state (e.g. *n*π*) be held liable for the observed 80 fs time constant in 5mUrd? We thoroughly investigated this possibility by re-computing the energetics along all trajectories, this time taking into consideration further ππ* and (the lowest) *n*π* states. *Ad hoc* non-adiabatic Tully fewest switches surface hopping dynamics in this new basis estimated that, even if 5mUrd spends a picosecond in the ππ* state, effectively it does not undergo non-adiabatic transfer to another excited state before reaching the CI seam with the ground state (Supplementary Note 3.5.2). This observation is supported by our measurements in the picosecond domain, which show that the spectral dynamics is concluded after few picoseconds (Supplementary Fig. S40). Moreover, it agrees with recent photoelectron spectroscopy experiments on thymine and 5mUrd which also did not find evidence for the involvement of the *n*π* state [28,37].

Somewhat surprisingly and in contrast with 5mUrd, we find that Urd is susceptible to a non-adiabatic transfer to the nearest nπ* state, despite its short ππ* lifespan. This behavior is attributed to the strong ππ*/*n*π* wavefunction mixing in the FC region and to the energetic proximity of the ππ* and the nπ* states that can occur along the dynamics (Supplementary Note 3.5.1). In Urd we estimate an upper limit of 20% for the yield of non-adiabatic transfer from the ππ* state to the nπ* state. This is experimentally confirmed by a long living signal detected at ~3.50 eV (Supplementary Figs. S36 and S37), also reported recently by Crespo and coworkers[29] and compatible with the calculated absorption signal of the np* state at ~3.10 eV in our previously reported static calculations[39]. It has been demonstrated recently that the fraction of the population that ends up in the nπ* state continues its evolution towards the triplet state manifold via an ISC on the nanosecond time scale[24].

Vibrational modes controlling the excited state dynamics of uridine and 5-methyluridine: signatures of the motion towards the CI

The sub-30-fs temporal resolution of our experimental setup reveals impulsively excited coherent oscillations in the SE signal (Figs. 1c and 2c), thereby allowing an unprecedented insight into the excited state vibrational dynamics of the nucleosides. By applying a high bandpass Fourier filter, we obtain the oscillatory component of the TA spectra (time traces at different probe photon energies shown in Fig. 3a). In both systems the oscillations are initiated immediately with the excitation. In Urd they decay on the 100-fs timescale (similarly to the SE) and exhibit only a few periods, strongly supporting the excited state

origin of the underlying vibrational dynamics. In 5mUrd, on the other hand, the coherent oscillations can be clearly resolved until 700 fs, in agreement with the much longer lifetime of the ππ* state.

A 2D Fourier analysis of the oscillatory component of the simulated SE signals (Figure 3b, lower panels) accurately reproduces the experimental 2D maps (Figure 3b, upper panels). The experimental maps of both Urd and 5mUrd reveal a dominant mode with a frequency of 750 cm^{-1}. The presence of a node around 3.80 eV, which coincides with the maximum of the SE band, and the observed »p phase shift between oscillations at probe photon energies to the red and the blue of this node, support the assignment of the coherence to the excited state[38]. This mode is clearly reproduced by the simulation, albeit at slightly lower frequency (~720 cm^{-1}); the same occurs for the node between 3.8-4.0 eV which closely matches the vertical energy gap at the pp* excited state minima of both nucleosides[37]. We also note the weak mode below 600 cm^{-1} present in the Urd map, whose amplitude is slightly overestimated in the simulation.

Excited state normal model analysis (NMA, see Supplementary Note 3.7 for more details) allows identifying the modes responsible for the coherent oscillations in the SE. In both systems, the 750 cm^{-1} mode is a breathing mode of the aromatic ring, characterized by a large amplitude of the $N_1C_6C_5$ angle (see insets in Fig. 3b). The ring breathing mode, together with high frequency C_5C_6 and CO stretching modes, which are beyond the limits of the temporal resolution of our experimental setup, dominate the excited state vibrational dynamics. The NMA demonstrates that in Urd photoexcitation delivers significant amount of vibrational energy in modes involving the C_5 and C_6 carbon atoms, eventually weakening the double bond and facilitating the ring puckering. NMA of Urd associates a frequency of 600 cm^{-1} to the hydrogen out-of-plane bending accompanying the puckering (see inset of Fig. 3b). Thus we assign the peak below 600 cm^{-1} observed in the experimental and theoretical Fourier transform maps of Urd to a signature of the coherent wavepacket motion towards the CI seam (Fig. 3b).

Conclusions

The unprecedented combination of TA spectroscopy with sub-30-fs time resolution in the UV and QM/MM simulations with highly correlated QM methods and explicit computation of spectroscopic signals, has allowed us to finally disclose the decay pathways in water-solvated Urd and 5mUrd. We conclude that: i) the sub-100-fs time constant dominating the spectral dynamics of Urd is associated with a coherent ballistic wave packet motion towards the $\pi\pi^*/S_0$ CI (Fig. 4a); ii) the two-component decay for 5mUrd is to be ascribed to the immediate motion away from the FC point (fast component) and the subsequent IC to the ground state (slow component); iii) the population of the dark np* state is only detected for Urd (Fig. 4a) and is not associated with the slower lifetime of 5mUrd. We identify ring puckering due to hydrogen (Urd) or methyl (5mUrd) out-of-plane bending as the main mechanism driving the evolution towards the CI and rationalize the difference in decay times with the larger inertia of the methyl group in 5mUrd. We link the enhanced photoreactivity of 5mUrd with respect to Urd to its longer excited state lifetime enabling the activation of specific reaction coordinates (Fig. 4b), elucidating the

origin of the lesion susceptibility of thymine-containing DNA strands. Eventually, we identify the experimentally detected 600 cm^{-1} coherent vibration as the signature of the H-out-of-plane mode accompanying the ring puckering in Urd during the motion towards the CI.

Methods

Experimental setup. Ultrafast TA experiments were carried out on a home-made pump-probe setup[34], based on a Ti:Sapphire laser (Libra, Coherent) delivering 100-fs pulses at 1.55 eV photon energy and 1 kHz repetition rate. A fraction of the laser power was used to feed a broadband visible non-collinear optical parametric amplifier (NOPA). The output pulses (1.77-2.38 eV), compressed to sub-10-fs duration by chirped dielectric mirrors, were successively frequency doubled in a 20-mm-thick Type I b-barium borate crystal, generating broadband UV pump pulses with spectrum spanning 4.43-4.6 eV. The UV pulses were compressed with a MgF_2 prism pair to nearly transform-limited 18-fs duration, characterized by two-dimensional spectral interferometry[35]. Broadband probe pulses, covering 1.9-3.9 and 3.5-4.6 eV, were obtained through white light continuum generation by focusing either the laser fundamental or its second harmonic in a slowly moving 2 mm-thick CaF_2 plate. The instrumental response function of the setup is estimated to be 25-35 fs, depending on the probe wavelength.

In order to avoid photodamage of the sample and generation of solvated electrons by two-photon absorption from water, the pump energy was limited to 20-30 nJ (resulting in a fluence of 88-132 $\mu J/cm^2$) and a laminar flowing jet configuration (~0.15 mm path length) was employed. TA spectra of the pure solvent are provided in the Supplementary Information. After the sample, the transmitted probe was sent to a spectrometer (SP2150 Acton, Princeton Instruments) and detected using a linear image sensor driven by a custom-built electronic board (Stresing Entwicklungsburo GmbH). For each probe wavelength, the differential absorption (ΔA) was measured as a function of the pump-probe delay. Measurements were recorded in parallel (main text), magic and orthogonal (Supplementary Note 5) pulse polarizations.

Sample preparation. 5-methyluridine (97% purity) and uridine (99% purity) were purchased from Sigma-Aldrich and used as received. A phosphate-buffered saline (PBS) solution was prepared by dissolving 3.6 g of sodium dihydrogen phosphate and 4.26 g of sodium hydrogen phosphate in ultrapure water to obtain a pH 7.4 and a concentration of 15 mM. The 5mUrd and Urd in PBS solutions were prepared to obtain concentrations respectively of 24.2 and 27.6 mM, resulting in an absorbance of 3 OD at the central pump wavelength. The steady-state absorption spectra are reported in the Supplementary Fig. 28.

Computational methods. Molecular dynamics simulations following Newton's equations of motion for the nuclei and utilizing hybrid QM/MM numerical gradients were performed at the full-π SS-2-CASPT2/SA-2-CASSCF(10,8) level of theory for 500 fs (Urd) and for 1000 fs (5mUrd) with a time step of 1.0 fs applying Tully's fewest switches surface hopping algorithm[39] with the Tully-Hammes-Schiffer (THS) scheme[40] and a decoherence correction as implemented by Persico et al.[41] (Supplementary Note 2.5). The state averaging covered the ground and the lowest ππ* state. A High/Medium/Low Layer (HL/ML/LL) partitioning was applied to a spherical droplet centered at the nucleoside with a radius of 12

Å. The HL (QM region) comprises the nucleobase. The sugar and water molecules in 5 Å distance from the center of mass of the nucleoside were included in the movable ML. The remaining water molecules were kept fixed in the LL. The generally contracted basis set ANO-L adopting valence double-ξ contractions was utilized[42].

The simulations were performed for 60 geometry realizations (per system) selected out of 500 snapshots generated via Wigner sampling (Supplementary Notes 2.3 and 3.1) on top of a representative geometry taken from a classical molecular mechanics simulation (Supplementary Note 2.1) and refined within the QM/MM framework at the Möller-Plesset second order perturbation theory (MP2, Supplementary Note 2.2). The geometry optimizations and simulations were conducted with the COBRAMM program[43], interfacing the QM software Molcas 8[44] with the AMBER suite of classical force fields[45]. Wigner sampling was realized with a stand-alone script, part of the program JADE[46]. On the basis of the simulations, TA spectra were generated (Supplementary Note 2.8) after computing the excited state electronic structure (energies and transition dipole moments) of Urd and 5mUrd at the SS-20-CASPT2/SA-20-CASSCF(10,8) level of theory at every time step along the trajectories.

We performed an extensive methodology benchmarking concerning the active space size (full-π vs. extended, Supplementary Note 3.3) and the choice of CASPT2 flavor (single-state vs. multi-state, Supplementary Notes 2.6 and 3.4). For stability reasons we could not obtain energy conservation during the molecular dynamics simulations when the oxygen lone pairs (and the associated nπ* states) are included in the active space. In order to estimate their involvement, we: a) analyzed the extent of ππ*/nπ* mixing in the FC region; b) analyzed the evolution of the energy gap between the lowest ππ* state and next higher lying excited states (two ππ* and two nπ*) along the computed trajectories; c) performed ad-hoc non-adiabatic Tully fewest switches surface hopping dynamics in a diabatic basis to resolve the percentage of trajectories that depart from the ππ* state before internal conversion to ground state (Supplementary Notes 2.7 and 3.5).

Online content

Any Nature Research reporting summaries, source data, extended data, supplementary information, acknowledgements, peer review information; details of author contributions and competing interests; and statements of data and code availability are available at https://doi.org/.....

References

1. Pfeifer, G. P. & Besaratinia, A. UV wavelength-dependent DNA damage and human non-melanoma and melanoma skin cancer. *Photochem. Photobiol. Sci.* **11**, 90–97 (2012).
2. Pfeifer, G. P., You, Y.-H. & Besaratinia, A. Mutations induced by ultraviolet light. *Mutat. Res. Mol. Mech. Mutagen.* **571**, 19–31 (2005).
3. Haiser, K. *et al.* Mechanism of UV-Induced Formation of Dewar Lesions in DNA. *Angew. Chemie Int. Ed.* **51**, 408–411 (2012).

4. Cadet, J., Grand, A. & Douki, T. Solar UV radiation-induced dna bipyrimidine photoproducts: Formation and mechanistic insights. *Top. Curr. Chem.* **356**, 249–275 (2015).
5. Markovitsi, D. UV-induced DNA Damage: The Role of Electronic Excited States. *Photochem. Photobiol.* **92**, 45–51 (2016).
6. Schreier, W. J., Gilch, P. & Zinth, W. Early Events of DNA Photodamage. *Annu. Rev. Phys. Chem.* **66**, 497–519 (2015).
7. Barbatti, M., Borin, A. C. & Ullrich, S. Photoinduced processes in nucleic acids. *Top. Curr. Chem.* **355**, 1–32 (2015).
8. Conti, I. *et al.* Multiple Electronic and Structural Factors Control Cyclobutane Pyrimidine Dimer and 6–4 Thymine–Thymine Photodimerization in a DNA Duplex. *Chem. - A Eur. J.* **23**, 15177–15188 (2017).
9. Giussani, A., Conti, I., Nenov, A. & Garavelli, M. Photoinduced formation mechanism of the thymine-thymine (6-4) adduct in DNA; A QM(CASPT2//CASSCF):MM(AMBER) study. *Faraday Discuss.* **207**, 375–387 (2018).
10. Wang, H. & Chen, X. How Does Thymine DNA Survive Ultrafast Dimerization Damage? *Molecules* **22**, 60 (2016).
11. Pecourt, J. M. L., Peon, J. & Kohler, B. Ultrafast internal conversion of electronically excited RNA and DNA nucleosides in water. *J. Am. Chem. Soc.* **122**, 9348–9349 (2000).
12. Pecourt, J.-M. L., Peon, J. & Kohler, B. DNA excited-state dynamics: Ultrafast internal conversion and vibrational cooling in a series of nucleosides. *J. Am. Chem. Soc.* **123**, 10370–10378 (2001).
13. Peon, J. & Zewail, A. H. DNA/RNA nucleotides and nucleosides: Direct measurement of excited-state lifetimes by femtosecond fluorescence up-conversion. *Chem. Phys. Lett.* **348**, 255–262 (2001).
14. Onidas, D., Markovitsi, D., Marguet, S., Sharonov, A. & Gustavsson, T. Fluorescence Properties of DNA Nucleosides and Nucleotides: A Refined Steady-State and Femtosecond Investigation. *J. Phys. Chem. B* **106**, 11367–11374 (2002).
15. Ullrich, S., Schultz, T., Zgierski, M. Z. & Stolow, A. Electronic relaxation dynamics in DNA and RNA bases studied by time-resolved photoelectron spectroscopy. *Phys. Chem. Chem. Phys.* **6**, 2796 (2004).
16. Hudock, H. R. *et al.* Ab Initio Molecular Dynamics and Time-Resolved Photoelectron Spectroscopy of Electronically Excited Uracil and Thymine. *J. Phys. Chem. A* **111**, 8500–8508 (2007).
17. Middleton, C. T. *et al.* DNA Excited-State Dynamics: From Single Bases to the Double Helix. *Annu. Rev. Phys. Chem.* **60**, 217–239 (2009).
18. Kohler, B. Nonradiative decay mechanisms in DNA model systems. *J. Phys. Chem. Lett.* **1**, 2047–2053 (2010).
19. Crespo-Hernández, C. E., Cohen, B., Hare, P. M. & Kohler, B. Ultrafast excited-state dynamics in nucleic acids. *Chem. Rev.* **104**, 1977–2019 (2004).

20. Conti, I. & Garavelli, M. Evolution of the Excitonic State of DNA Stacked Thymines: Intrabase ππ* → S 0 Decay Paths Account for Ultrafast (Subpicosecond) and Longer (>100 ps) Deactivations. *J. Phys. Chem. Lett.* **9**, 2373–2379 (2018).
21. Improta, R., Santoro, F. & Blancafort, L. Quantum Mechanical Studies on the Photophysics and the Photochemistry of Nucleic Acids and Nucleobases. *Chem. Rev.* **116**, 3540–3593 (2016).
22. Kobayashi, T. & Kida, Y. Ultrafast spectroscopy with sub-10 fs deep-ultraviolet pulses. *Phys. Chem. Chem. Phys.* **14**, 6200 (2012).
23. Prokhorenko, V. I., Picchiotti, A., Pola, M., Dijkstra, A. G. & Miller, R. J. D. D. New Insights into the Photophysics of DNA Nucleobases. *J. Phys. Chem. Lett.* **7**, 4445–4450 (2016).
24. Gustavsson, T., Sharonov, A. & Markovitsi, D. Thymine, thymidine and thymidine 5'-monophosphate studied by femtosecond fluorescence upconversion spectroscopy. *Chem. Phys. Lett.* **351**, 195–200 (2002).
25. Cohen, B., Crespo-Hernández, C. E. E. & Kohler, B. Strickler–Berg analysis of excited singlet state dynamics in DNA and RNA nucleosides. *Faraday Discuss.* **127**, 137–147 (2004).
26. Buchner, F., Nakayama, A., Yamazaki, S., Ritze, H.-H. & Lübcke, A. Excited-state relaxation of hydrated thymine and thymidine measured by liquid-jet photoelectron spectroscopy: Experiment and simulation. *J. Am. Chem. Soc.* **137**, 2931–2938 (2015).
27. Gustavsson, T., Banyasz, A., Improta, R. & Markovitsi, D. Femtosecond fluorescence studies of DNA/RNA constituents. *J. Phys. Conf. Ser.* **261** (2011).
28. Erickson, B. A. *et al.* Relaxation Dynamics of Hydrated Thymine, Thymidine, and Thymidine Monophosphate Probed by Liquid Jet Time-Resolved Photoelectron Spectroscopy. *J. Phys. Chem. A* **123**, 10676–10684 (2019).
29. Brister, M. M. & Crespo-Hernández, C. E. Excited-State Dynamics in the RNA Nucleotide Uridine 5'-Monophosphate Investigated Using Femtosecond Broadband Transient Absorption Spectroscopy. *J. Phys. Chem. Lett.* **10**, 2156–2161 (2019).
30. Xue, B., Yabushita, A. & Kobayashi, T. Ultrafast dynamics of uracil and thymine studied using a sub-10 fs deep ultraviolet laser. *Phys. Chem. Chem. Phys.* **18**, 17044–17053 (2016).
31. Hare, P. M., Crespo-Hernandez, C. E. & Kohler, B. Internal conversion to the electronic ground state occurs via two distinct pathways for pyrimidine bases in aqueous solution. *Proc. Natl. Acad. Sci.* **104**, 435–440 (2007).
32. Pollum, M., Martínez-Fernández, L. & Crespo-Hernández, C. E. Photochemistry of Nucleic Acid Bases and Their Thio- and Aza-Analogues in Solution. in *Top Curr Chem* 245–327 (Springer, 2014).
33. Gustavsson, T. *et al.* Singlet excited-state behavior of uracil and thymine in aqueous solution: A combined experimental and computational study of 11 uracil derivatives. *J. Am. Chem. Soc.* **128**, 607–619 (2006).
34. Borrego-Varillas, R., Ganzer, L., Cerullo, G. & Manzoni, C. Ultraviolet Transient Absorption Spectrometer with Sub-20-fs Time Resolution. *Appl. Sci.* **8**, 989 (2018).

35. Borrego-Varillas, R. *et al.* Optimized ancillae generation for ultra-broadband two-dimensional spectral-shearing interferometry. *JOSA B* **32**, 1851–1855 (2015).
36. Pepino, A. J., Segarra-Martí, J., Nenov, A., Improta, R. & Garavelli, M. Resolving Ultrafast Photoinduced Deactivations in Water-Solvated Pyrimidine Nucleosides. *J. Phys. Chem. Lett.* **8**, 1777–1783 (2017).
37. Wolf, T. J. A. *et al.* Observation of Ultrafast Intersystem Crossing in Thymine by Extreme Ultraviolet Time-Resolved Photoelectron Spectroscopy. *J. Phys. Chem. A* **123**, 6897–6903 (2019).
38. Kumar, A. T. N., Rosca, F., Widom, A. & Champion, P. M. Investigations of amplitude and phase excitation profiles in femtosecond coherence spectroscopy. *J. Chem. Phys.* **114**, 701 (2001).
39. Tully, J. C. Mixed quantum–classical dynamics. *Faraday Discuss.* **110**, 407–419 (1998).
40. Hammes-Schiffer, S. & Tully, J. C. Proton transfer in solution: Molecular dynamics with quantum transitions. *J. Chem. Phys.* **101**, 4657–4667 (1994).
41. Granucci, G. & Persico, M. Critical appraisal of the fewest switches algorithm for surface hopping. *J. Chem. Phys.* **126**, 134114 (2007).
42. Widmark, P.-O., Malmqvist, P. & Roos, B. O. Density matrix averaged atomic natural orbital (ANO) basis sets for correlated molecular wave functions. *Theor. Chim. Acta* **77**, 291–306 (1990).
43. Weingart, O. *et al.* COBRAMM 2.0 — A software interface for tailoring molecular electronic structure calculations and running nanoscale (QM/MM) simulations. *J. Mol. Model.* **24**, 271 (2018).
44. Aquilante, F. *et al.* Molcas 8: New capabilities for multiconfigurational quantum chemical calculations across the periodic table. *J. Comput. Chem.* **37**, 506–541 (2016).
45. Salomon-Ferrer, R., Case, D. A. & Walker, R. C. An overview of the Amber biomolecular simulation package. *Wiley Interdiscip. Rev. Comput. Mol. Sci.* **3**, 198–210 (2013).
46. Du, L. & Lan, Z. An On-the-Fly Surface-Hopping Program JADE for Nonadiabatic Molecular Dynamics of Polyatomic Systems: Implementation and Applications. *J. Chem. Theory Comput.* **11**, 1360–1374 (2015).

Declarations

Data availability

Data generated or analysed during this study are included in this Article (and its Supplementary Information). Source data are available from the corresponding authors upon reasonable request.

Code availability

The analysis codes used to generate the data presented in this study are available from the corresponding authors upon reasonable request.

Acknowledgements

We thank Dr. Stefano Santabarbara for preparing the PBS. P.K., G.C. and M.G. acknowledge support from the H2020 Grant Agreement number 765266 (LightDyNAmics). G.C. and M.G. acknowledge support from the European Research Council Advanced Grant STRATUS (ERC-2011-AdG No. 291198) and RBV from the Marie Curie Actions (grant n. 328110). M.G. acknowledges support from PRIN 2017 project PHANTOMS, Prot. 2017A4XRCA. I.R. and M.G. acknowledge the Agence National de la Recherche project FEMTO-2DNA (ANR-15-CE-29-0010). The authors acknowledge the use of HPC resources of the “Pôle Scientifique de Modélisation Numérique” at the ENS-Lyon, France.

Author contributions

RBV, AO, PK and CM built the experimental setup. PK, RBV, AO, LG and ID performed the measurements. AN and OW implemented the non-adiabatic dynamics algorithm. AN performed the simulations. RBV, AN, PK, IC and IR analysed the data. GC and MG conceived the idea and supervised the project. RBV and AN wrote the manuscript with inputs from all the authors.

Competing interest

The authors declare no competing interests.

Additional information

Supplementary information is available for this paper at

Correspondence and requests for materials should be addressed to Prof. Giulio Cerullo (giulio.cerullo@polimi.it) or Prof. Marco Garavelli (marco.garavelli@unibo.it)

Reprints and permissions information is available at www.nature.com/reprints

Figures

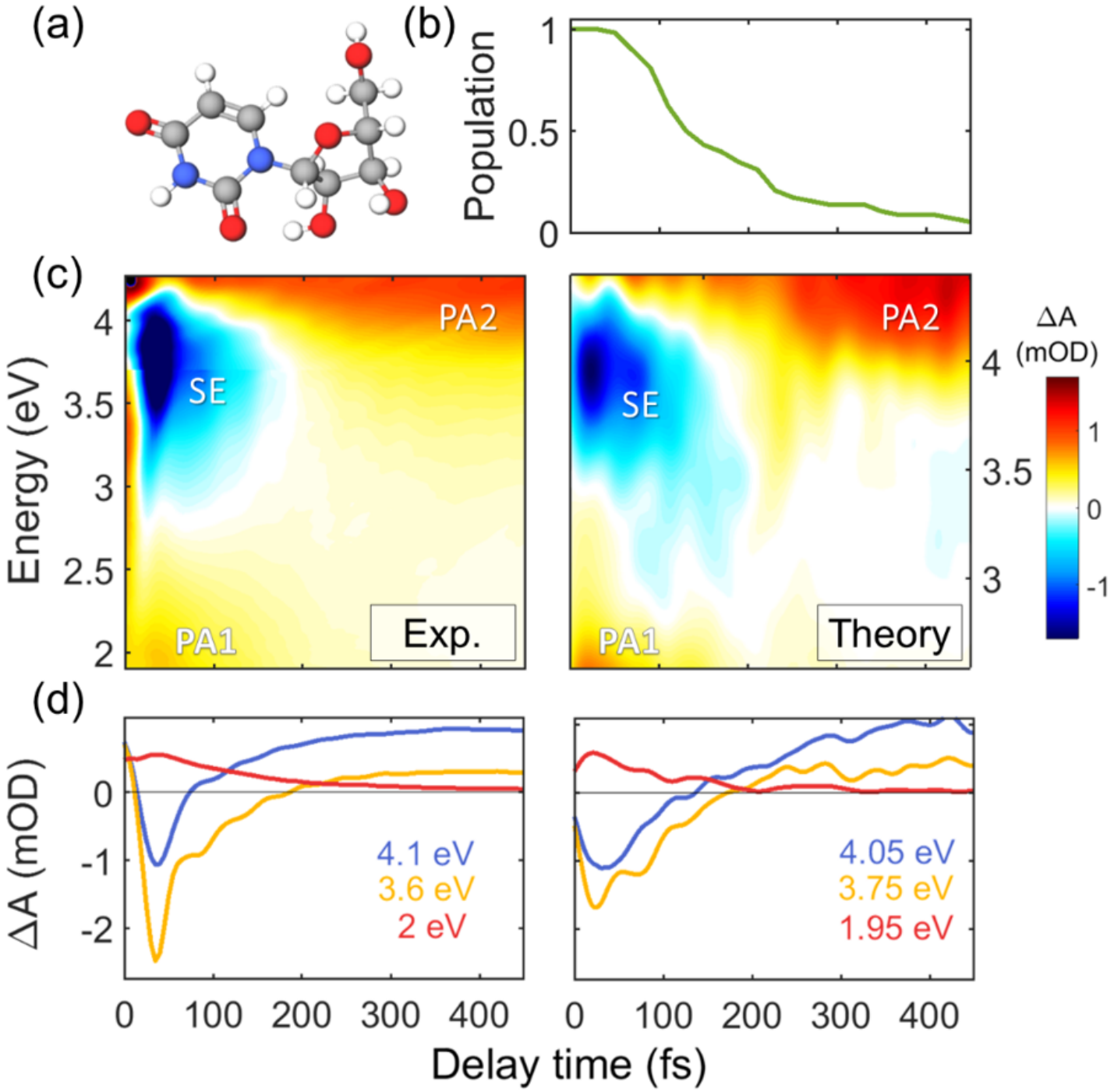

Figure 1

Excited state dynamics of uridine. (a) Molecular structure of Urd. (b) Time-dependent excited state population calculated by QM/MM simulations. (c) Experimental (left) and computed (right) TA maps of Urd. Two photo-induced absorption bands (labelled PA1 and PA2) and a stimulated emission (SE) band can be identified. (d) TA dynamics at selected probe photon energies.

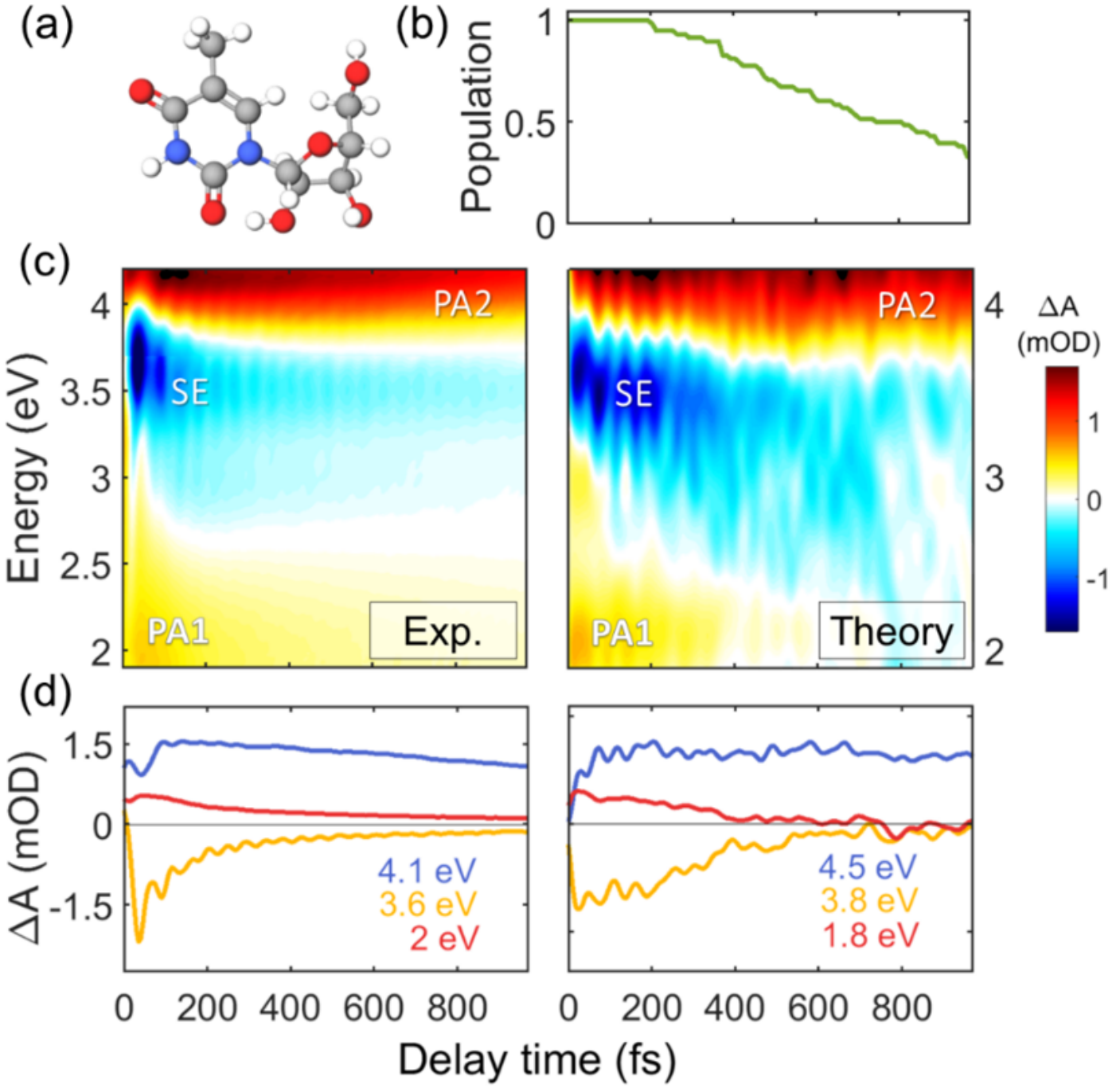

Figure 2

Excited state dynamics of 5-methyluridine. (a) Molecular structure of 5mUrd. (b) Time-dependent excited-state population calculated by QM/MM simulations. (c) Experimental (left) and computed (right) TA maps of 5mUrd. Two photo-induced absorption bands (labelled PA1 and PA2) and a stimulated emission (SE) band can be identified. (d) TA dynamics at selected probe photon energies.

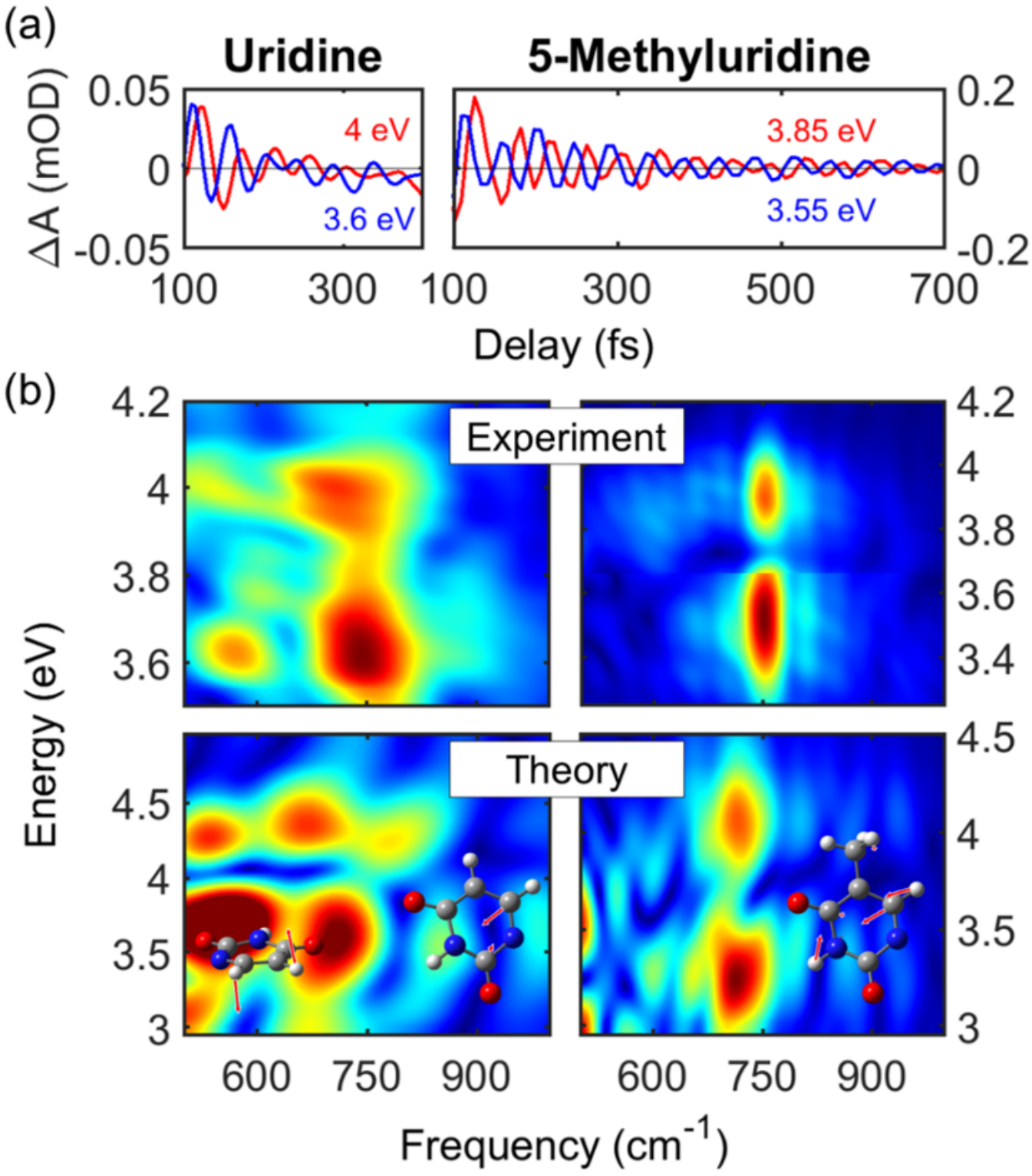

Figure 3

Coherent vibrations in pyrimidines. (a) Oscillatory patterns were obtained after subtraction of the slowly varying component from the transient spectra maps by employing a bandpass Fourier filter. Two examples of the extracted oscillatory dynamics are shown for Urd (left panel) and 5mUrd (right panel). (b) Comparison of the experimental and theoretical two-dimensional Fourier transform maps of the residuals (oscillations) for Urd (left panels) and 5mUrd (right panels; the colour jump in the experimental map is

due to the merge of the two measurements corresponding to two different probe spectral regions). Inset left panel: schemes of the 600 cm-1 (right) and 750 cm-1 (left) vibrational modes in Urd. Inset right panel: scheme of the 750 cm-1 vibrational mode in 5mUrd.

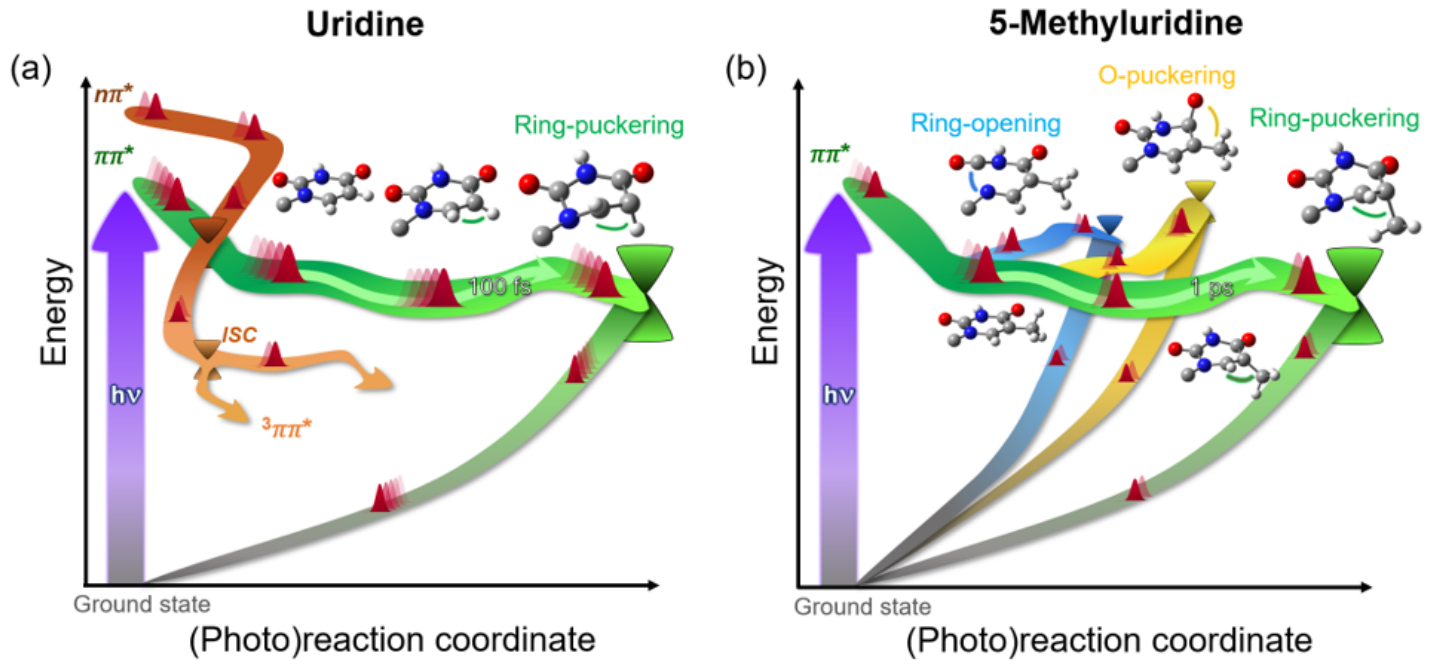

Figure 4

Excited state decay pathways in pyrimidines. Schematic representations of photoinduced events in (a) Urd and (b) 5mUrd, showing similar PES (in green) from the FC region of the bright ππ* state to the CI with S0 for the two systems. While faster wave packet dynamics and partial population of the nπ* state are associated with Urd, slower dynamics due to the methyl-substitution and access to multiple deactivation pathways are observed in 5mUrd.

Supplementary Files

This is a list of supplementary files associated with this preprint. Click to download.

- VarillasnucleosidesSI.pdf